Formation and interaction of ferromagnetic clusters in antiferromagnetic $YBa_2Cu_3O_{6+x}$ films

S. L. Gnatchenko and A. M. Ratner
B. Verkin Institute for Low Temperature Physics and Engineering, National Academy of Sciences of Ukraine, 310164 Kharkov, Ukraine

M. Baran, R. Szymczak, and H. Szymczak
Institute of Physics, Polish Academy of Sciences, Aleja Lotników 32/46, 02-668 Warsaw, Poland
(Received 12 August 1996; revised manuscript received 1 October 1996)

The magnetization of $YBa_2Cu_3O_{6+x}$ antiferromagnetic films was experimentally studied as a function of magnetic field, temperature, oxygen index, and photoillumination dose. The results are evidence of the formation of ferromagnetic clusters, promoted by oxygen holes, in a general accordance with the phase separation approach. However, field and concentration dependences of magnetization display some essential features which can be explained only with allowance for the motion of holes in long-distance potential wells, created in the CuO_2 plane (where the clusters are formed) by charged copper-oxygen chains (allocated in the CuO_x plane where excess oxygen ions are incorporated). A significant straggling of ferromagnetic clusters over sizes (from 100 to 10^4 or more spins per cluster) was discovered, the properties of clusters being essentially dependent on their size. [S0163-1829(97)04405-6]

I. INTRODUCTION AND PROBLEM STATEMENT

During past years, the magnetic structure of $YBa_2Cu_3O_{6+x}$ (YBCO) dielectrics was an object of rather intensive studies.[1–8] The problem is complicated enough and from the nowaday point of view consists mainly in the following.

At $x=0$, a $YBa_2Cu_3O_{6+x}$ crystal is known to be an antiferromagnet (AFM) (with copper spins antiferromagnetically ordered within the CuO_2 plane, with the exchange integral $J_{AFM}\sim 0.1$ eV). The AFM exchange of two Cu^{2+} ions is realized through the chemically inactive closed-shell O^{2-} ion lying between them. With an increase of x, in the CuO_2 plane oxygen holes appear which locally destroy the AFM ordering. An oxygen ion with a trapped hole (O^- with the configuration of chemically active Cl) strongly interacts with two adjacent Cu^{2+} ions. The interaction energy is minimized if the O^- and Cu^{2+} spins are antiparallel, so that the spins of the involved copper ions are parallel to each other. So, in the presence of an oxygen hole the effective exchange energy of Cu^{2+} spins, J_{FM} has the opposite sign and a much greater magnitude as compared to J_{AFM}.[9–11] J_{FM} is of the order of a chemical bond energy, i.e., a few electron volts. It follows that one delocalized hole can destroy the AFM ordering of a large number ($\sim|J_{FM}/J_{AFM}|$) of copper spins.

With an increase of x and of hole concentration, the tendency to the ferromagnetic (FM) ordering grows and entails the formation of FM clusters in the CuO_2 plane. This phenomenon was treated in the terms of phase separation.[12–18] According to this approach, it is energetically favorable for oxygen holes to concentrate in some regions and organize their ferromagnetic microphase, whereas the AFM phase persists in the rest of material depleted in holes.

Some indications on a latent ferromagnetism, i.e., the existence of spatial regions with a nonzero magnetic moment, appeared even in early papers concerning the magnetic properties of YBCO crystals.[1–3] The second magnetic transition close to 40 K, as well as a strongly nonlinear field dependence of magnetization at low temperatures, were associated with a latent ferromagnetism.[1,2,6–8] Recently, the authors[19] have obtained quite distinct evidences of the existence of FM clusters in YBCO dielectrics. In general features, these experimental data agree with the conception of phase separation.[12–18]

However, some essential regularities, experimentally observed in Ref. 19, cannot be explained within the phase separation approach in its present form. For instance, the magnetic susceptibility of $YBa_2Cu_3O_{6+x}$ insulators grows with x only for $x<0.3$ and diminishes with increasing x for $x>0.39$ despite a fast attendant increase of the number of holes. The conception of phase separation is also insufficient to explain the field dependence of magnetization in a wide range of magnetic fields. These (and some other) qualitative discrepancies indicate on the existence of un unknown additional mechanism involved in the formation of FM clusters in YBCO insulators.

The present paper is concerned with the identification of such mechanism. With that end in view, the authors drew attention to another sphere of phenomena common for $YBa_2Cu_3O_{6+x}$ crystals. It is well known[20] that excess oxygen ions (x ions per unit cell) form charged copper-oxygen chains $Cu^{2+}O^{2-}Cu^{2+}\cdots O^{2-}Cu^{2+}$ in the CuO_x plane that is parallel to the CuO_2 plane. As was shown in Ref. 21 and in Ref. 22, hole movement and electronic properties are essentially affected by the long-distance modulation of Coulomb potential, produced in the CuO_2 plane by the chains (even a point excess charge lying in the CuO_x plane creates in the CuO_2 plane a potential well with the halfwidth seven times exceeding the interatomic distance). For instance, the insulator-metal transition (observed at $x\approx 0.42$) is connected with the concentration evolution of the long-distance potential. In the insulating phase ($x<0.42$) oxygen holes are localized in long-distance wells. As oxygen content, x, increases, the chains lengthen, the wells broaden, and the mobility threshold of holes lowers. Simultaneously the number of holes in the CuO_2 plane grows, and at $x\approx 0.42$ their

Fermi level intersects the mobility threshold.

As it is shown below, the formation of FM clusters is closely connected with the concentration and motion of holes in the long-distance potential wells. In order to explore this sphere of phenomena, we shall, first, experimentally examine magnetic properties of YBCO insulators with a particular attention to all the anomalous features from the point of view of the phase separation approach (Sec. II). All the qualitative discrepancies between the experiment and this approach are pointed out in Sec. II via the primary analysis of the experimental results. Based on these data, we shall develop in Sec. III the simplest theory, which complement the phase separation conception by taking into account peculiarities of hole motion in long-distance potential wells. The theory will naturally explain all the illusive anomalies in the observed magnetic properties (Sec. IV).

II. EXPERIMENTAL RESULTS AND THEIR PHYSICAL MEANING

We have performed measurements of the field and temperature dependences of magnetization of $YBa_2Cu_3O_{6+x}$ films with various oxygen content. The magnetization was measured by a superconducting quantum interference device (SQUID) magnetometer (MPMS Quantum Design) in magnetic field which was varied in the interval $0<H<50$ kOe and directed parallel or perpendicular to the c axis. The measurements were carried out in the temperature range $4.5<T<150$ K.

The $YBa_2Cu_3O_{6+x}$ films (about 150 nm thick) were deposited by laser ablation on the (001) $SrTiO_3$ substrates 0.3 mm thick. The c axis of the films is normal to their surface. YBCO films of the mentioned thickness are transparent to visible light which renders the possibility to expose them to a uniform photoillumination. Another advantage of thin films consists in an easy possibility to change oxygen content by annealing in vacuum.

In the initial state before annealing, all the films were superconducting with the transition temperature $T_c=88$ to 90 K, which corresponds to oxygen index $x=0.9$ to 1. A small transition width (of about 1 K) provided evidence for a high degree of perfection and homogeneity of the samples. The samples with the required lowered oxygen content were prepared by annealing at the temperature 300–330 °C in vacuum (about 10^{-2} mm Hg) under permanent evacuation. The oxygen content x in the annealed films was determined independently in two ways. First, the lattice parameter c of the films was measured by x-ray diffraction method, and the c-versus-x dependence, given in Refs. 23 and 24, was used. Second, x was inferred from the superconducting transition temperature T_c with the use of its concentration dependence taken from Ref. 25. T_c was found from the temperature dependence of the magnetization of the film, measured in low magnetic fields, and from the temperature dependence of its electrical conductivity σ. For the films in the insulating (nonsuperconducting) phase, oxygen content was determined using the x-ray data and the measured $\sigma(T)$ dependence with allowance for its concentration evolution.[23]

To provide the possibility of the simultaneous magnetic and electric measurements, two samples of area of about 0.1 cm^2 were initially cut from the same film and silver contacts were deposited on one of them. Then both the samples were annealed simultaneously under the same conditions. After the annealing, the contact-free sample was used for magnetic measurements and the sample with silver contacts for the measurements of electric conductivity by the four probe method.

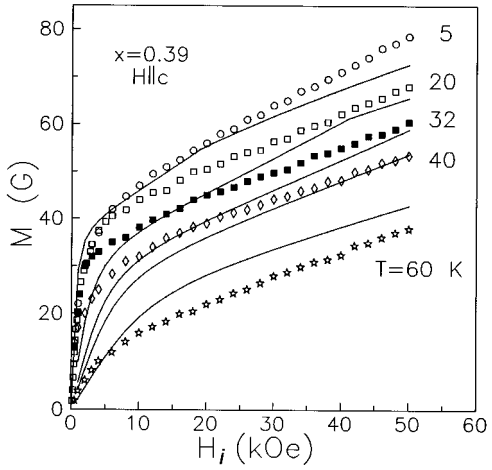

FIG. 1. Field dependences of magnetization of the $YBa_2Cu_3O_{6+x}$ film with $x\approx0.39$ for $\mathbf{H}\|c$ at various temperatures. Solid curves were calculated using Eq. (13).

The metal-insulator transition in the examined films was observed at $x\approx0.42$. The temperature dependence of the electrical conductivity of the film with $x\approx0.39$ was typical of a semiconductor ($\sigma_{300}/\sigma_{4.2}\approx21$). The dependence $\sigma(T)$ of the film with $x\approx0.41$ was of metal type ($\sigma_{300}/\sigma_{4.2}\approx0.2$) but the transition to superconducting state was not observed in this film even at the liquid helium temperature. The film with $x\approx0.44$ had superconducting transition at $T_c\approx10$ K.

The field and temperature dependences of magnetization were investigated for the films with oxygen content in the range $0.2<x<0.6$. The total magnetic moment of a $YBa_2Cu_3O_{6+x}$ film together with the $SrTiO_3$ substrate was measured. The magnetic moment of the film was determined by subtracting the diamagnetic contribution of the substrate from the measured value of the total magnetic moment. For this purpose, the magnetic susceptibility of the pure $SrTiO_3$ substrate was measured and found to be equal to -1.13×10^{-7} emu/Oe g.

A. Field dependences of magnetization and cluster size. Nonmonotone concentration dependence of susceptibility

The field dependences, $M(H)$, of the magnetization of annealed $YBa_2Cu_3O_{6+x}$ films were measured upon cooling the film to required temperature in zero magnetic field (between the consecutive measurements the sample was heated up to 100 K). The $M(H)$ curves were measured in the course of increasing the field from 0 up to 50 kOe and of its subsequent decrease down to zero.

First we focus attention on the concentration point $x\approx0.39$, which relates to the insulating AFM-ordered phase but provides large enough magnetization to be examined in detail when varying field and temperature. Figure 1 shows several $M(H)$ dependences measured at different tempera-

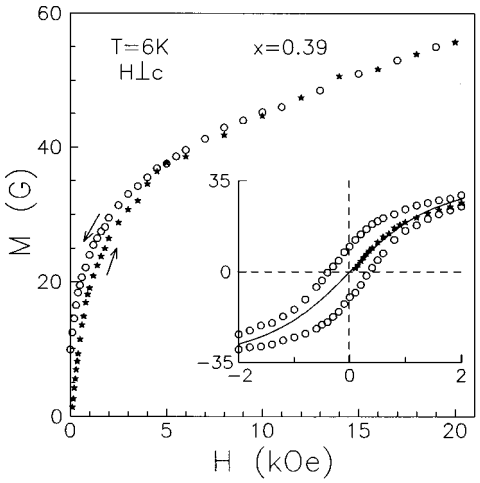

FIG. 2. Field dependences of magnetization of the $YBa_2Cu_3O_{6+x}$ film with $x \approx 0.39$ measured at $T=6$ K in increasing and decreasing magnetic field $\mathbf{H} \perp c$. The hysteresis loop of magnetization is shown in the inset, where Eq. (2) with $m_{\mathrm{clu}}=1.4\times10^{-18}$ G cm^3 is plotted by solid line.

tures in the field parallel to the c axis. The figure presents the measurements in increasing field. The abscissa is the internal field

$$H_i = H - 4\pi N_d M, \tag{1}$$

with the demagnetizing factor N_d. In this way account is taken of the demagnetization effect which is noticeable for small H if $\mathbf{H}$ is parallel to the c axis [in this case the demagnetizing factor N_d in Eq. (1) is close to unity whereas it turns to zero for the in-plane orientation of $\mathbf{H}$].

Similar $M(H)$ dependences were obtained also for $\mathbf{H} \perp c$. In this case the field dependences of magnetization, plotted in the axes M versus $H=H_i$, practically coincide with the curves of Fig. 1.

As an example, Fig. 2 presents the H dependence of magnetization for the in-plane orientation of $\mathbf{H}$ at $T=6$ K. The figure shows the $M(H)$ curves measured in increasing and decreasing field. These curves coincide within the error of measurements in the region $H>8$ kOe, while in lower fields a hysteresis is observed. The hysteresis loop of magnetization is shown in the inset of Fig. 2. The magnetization of a film does not vanish after decreasing the field down to zero. The remanent magnetization, M_r, reaches about 9 G for $x \approx 0.39$ at liquid helium temperature. With raising temperature the remanent magnetization diminishes and at $T>50$ K becomes less than 1 G. At low temperatures, the remanent magnetization persists for a long time. The remanent magnetization was observed in all of the examined nonsuperconducting films, the maximum being achieved at $x \approx 0.39$.

Before analyzing the presented results, let us show that the observed magnetization should be attributed to FM clusters. Indeed, the contribution of the AFM phase to magnetic susceptibility is $\chi_{\mathrm{AFM}} \sim M_{\mathrm{tot}}\mu / J_{\mathrm{AFM}} \sim 10^{-5}$ ($M_{\mathrm{tot}} \sim$ 300 G is the total magnetic moment of copper ions per unit volume, $\mu \approx 1.9\mu_B$ is the moment of one Cu^{2+} ion,[26] μ_B is the Bohr magneton, $J_{\mathrm{AFM}} \sim$ 0.1 eV is the AFM exchange energy). The observed susceptibility, estimated from the data presented in Fig. 1, is at least two orders of magnitude greater.

The moments of copper ions, belonging to the CuO_x plane, should also be taken into account. If their orientation is not fixed by the crystalline field, they make a paramagnetic contribution to susceptibility $\chi_{\mathrm{para}} \sim (\mu/3T)(M_{\mathrm{tot}}/3)$. Even at 5 K, χ_{para} does not exceed 10^{-3} which is twenty times less than the observed susceptibility in the region of low fields. In the region of strong fields, the observed slope of the magnetization curves (Fig. 1) is almost independent of temperature for $5<T<60$ K and therefore cannot be assigned to χ_{para} (although at 5 K χ_{para} is near to the observed slope).

Based on these considerations, the observed field dependence of magnetization should be assigned to FM clusters.

With this in view, let us consider the physical meaning of the magnetization curves presented in Fig. 1. The curves exhibit two contributions drastically different in the character of field behavior. One of them (called below the first contribution) increases rapidly with H and achieves saturation in low fields. The second contribution manifests itself in strong fields and slowly (almost linearly) grows with increasing field. As it is seen from Fig. 1, the second contribution is nearly independent of temperature below 60 K, whereas the first contribution noticeably decreases with raising temperature. The saturation value, M_s, of the first contribution (obtained via extrapolating the linear part of the magnetization curve to $H=0$) fast diminishes with raising temperature up to 55 K and slowly decreases with a further increase of temperature (see Fig. 9 of Ref. 19).

Now we will analyze the field dependence of the first contribution in order to derive the magnetic moment, m_{clu}, of a FM cluster. As was pointed out, the observed magnetization practically does not depend on the magnetic field orientation. It follows that the energy of the interaction between a cluster and the lattice is independent of the cluster moment orientation. So, magnetic field $\mathbf{H}$ turns the magnetic moments of noninteracting clusters similarly to those of free paramagnetic atoms with large classical moments and produces the equilibrium magnetization

$$M = M_s\{\coth(m_{\mathrm{clu}}H/T) - T/m_{\mathrm{clu}}H\}, \quad M_s = n m_{\mathrm{clu}}, \tag{2}$$

where n is the number of clusters per unit volume.

Fitting Eq. (2) to the experimental $M(H)$ dependence plotted in the inset of Fig. 2, we obtain the magnetic moment of a cluster at T = 6 K: $m_{\mathrm{clu}}=1.4\times10^{-18}$ G cm$^3=150\mu_B$. The straggling, corresponding to hysteresis, is small, since the nonequilibrium contribution to magnetization (considered in Sec. II B) is actually frozen at low temperatures in low fields. (With raising temperature the nonequilibrium contribution becomes unfrozen which hinders the use of the magnetization curves, related to higher temperatures, for the estimation of m_{clu}.) Taking for the atomic moment $\mu=1.9\mu_B$, the number of copper ions in a cluster is $N \approx 80$. Clusters with $N \approx 100$ (called normal-size clusters in contrast to giant clusters with $N \approx 10^4$ considered below) make a dominant contribution to magnetization for $T<40$ K [at higher temperatures normal-size clusters are destroyed, judging from a strong temperature decrease of M_s Ref. 19].

The magnetization magnitude of $YBa_2Cu_3O_{6+x}$ films depends on oxygen content. Figure 3 shows the x dependences of magnetization. As it is seen from Fig. 3, for low temperatures ($T=20$ K) the magnetization depends on x nonmonoti-

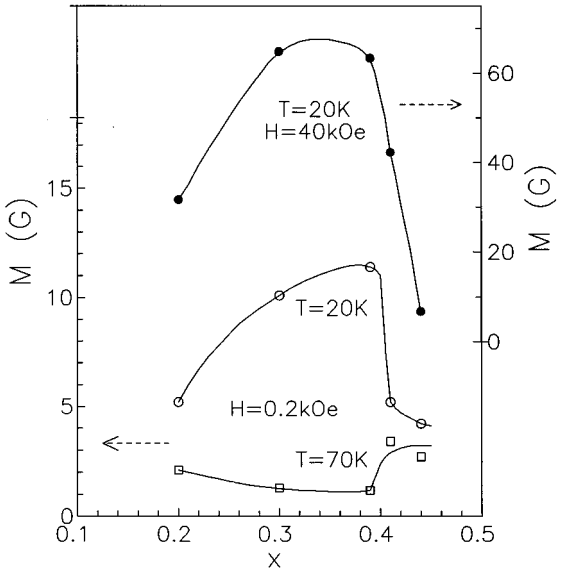

FIG. 3. Concentration dependences of magnetization in the fields 40 kOe and 200 Oe perpendicular to c axis. Two upper curves relate to the temperature point $T=20$ K and the lower curve to $T=70$ K (main contribution to magnetization is made by normal-size clusters in the former case and by very large clusters in the latter). Lines are guides for the eyes.

cally and in a similar way in low and strong fields. In the interval $0.2<x<0.3$ the magnetization increases with x more than twofold. As x raises from 0.30 to 0.39, the magnetization remains practically invariable. A further increase of x results in a sharp decrease of magnetization. Note that the concentration of holes rapidly grows with x in the total examined interval of concentrations, in particular just in the vicinity of the insulator-metal transition where magnetization sharply diminishes with raising x. Indeed, the conductivity of the film, measured at 4.2 K, grows from 1.2×10^3 $\Omega^{-1}\,\mathrm{m}^{-1}$ to $2.5\times10^5\Omega^{-1}\,\mathrm{m}^{-1}$ and to infinity (superconductance) as x varies from 0.39 to 0.41 and to 0.44, respectively.

B. Temperature dependence of magnetization. Manifestations of very large clusters

Magnetization curves presented in Fig. 1 reveal an unusual behavior in the region of low fields where their slope is almost independent of temperature up to 40 K. As it is shown below, this feature originates from a nonequilibrium contribution to magnetization in low fields. In order to explore such nonequilibrium phenomena, the temperature dependence of magnetization was examined in fixed low fields applied parallel or perpendicular to the c axis.

The measurements of magnetization were carried out in the course of heating of the sample which was cooled before to the liquid helium temperature in zero magnetic field [the $M_{\mathrm{ZFC}}(T)$ dependences] and in the course of cooling of the sample in magnetic field [the $M_{\mathrm{FC}}(T)$ dependences].

Figure 4, related to the magnetically ordered film with $x\approx0.39$ (nonsuperconducting), shows typical $M_{\mathrm{ZFC}}(T)$ and $M_{\mathrm{FC}}(T)$ dependences. A clearly manifested difference between the $M_{\mathrm{ZFC}}(T)$ and $M_{\mathrm{FC}}(T)$ curves evidences for a non-

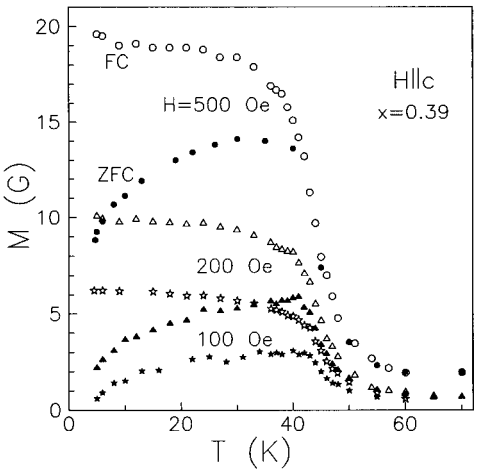

FIG. 4. Temperature dependences of ZFC (full symbols) and FC (open symbols) magnetization of the $YBa_2Cu_3O_{6+x}$ film with $x\approx0.39$ in the field $\mathbf{H}\|c$ of the various field strength.

equilibrium state of the magnetic subsystem (the equilibrium magnetization depends only on H and T). During the cooling of the film in magnetic field, the magnetization M_{FC} increases rapidly in the temperature interval $40<T<50$ K and significantly slower with a further lowering of temperature. When the film, which was cooled before in the absence of field, is heated in magnetic field, the magnetization M_{ZFC} increases with temperature up to about 40 K in the course of approaching of the thermodynamic equilibrium (at helium temperature M_{ZFC} was frozen at a low nonequilibrium value). With a further increase of temperature in the region of thermodynamic equilibrium ($T>40$ K), M_{ZFC} rapidly diminishes, being practically coincident with M_{FC}.

At low temperatures M_{ZFC} and M_{FC} differ significantly. As magnetic field increases, the relative difference $(M_{\mathrm{FC}}-M_{\mathrm{ZFC}})/M_{\mathrm{FC}}$ diminishes (i.e., the magnetic subsystem approaches equilibrium). At $H>8$ kOe the complete equilibrium is achieved and the difference between the curves $M_{\mathrm{ZFC}}(T)$ and $M_{\mathrm{FC}}(T)$ disappears. A similar behavior of magnetization was observed for all of the examined films with different oxygen indices x related to the nonsuperconducting magnetically ordered state.

For the reason given below, the nonequilibrium contribution to magnetization should be assigned to large clusters with the moment $m_{\mathrm{lar}}\gg m_{\mathrm{clu}}$. Let us estimate m_{lar} proceeding from the assumption that the nonequilibrium contribution is responsible for the fact that the magnetization curves, plotted in Fig. 1 at the temperatures 5, 20, 32, and 40 K, have equal slopes in the region of low fields. In this region magnetization consists of the equilibrium and nonequilibrium contributions, produced by normal-size and large clusters, respectively, and can be presented in the form $M=M_s(Hm_{\mathrm{clu}}/3T)+AM_{\mathrm{lar}}(Hm_{\mathrm{lar}}/3T)$ with the multiplier A depending on the degree of equilibrium. With regard to the above analysis of Fig. 4, one can put $A=0$ at 5 K and $A\approx1$ at 40 K. As it is seen from Fig. 1, $M_s\approx$ 40 G at 5 K and 25 G at 40 K. The saturation magnetization M_{lar}, produced by large clusters, can be estimated from the data presented in Fig. 1 as the ordinate of the point where the curve, related to 40 K, sharply changes its slope: $M_{\mathrm{lar}}\approx$ 15 G

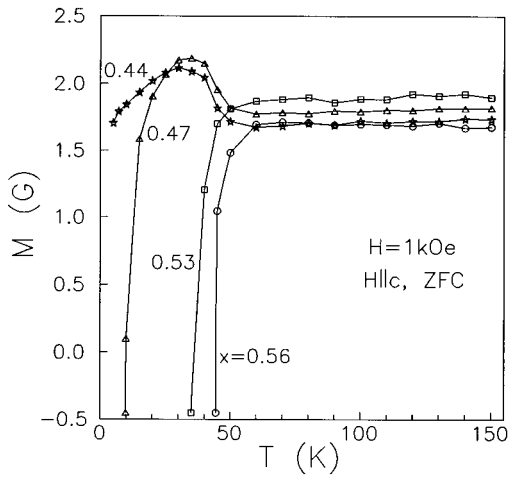

FIG. 5. Temperature dependences of ZFC magnetization of the $YBa_2Cu_3O_{6+x}$ films with different oxygen content x measured in the field $\mathbf{H}\|c$ of the strength 1 kOe.

(roughly the same estimation can be achieved from the data given in Fig. 4). Equating the slopes dM/dH at the temperatures 5 K and 40 K to each other, we obtain the estimation $m_{\rm lar}\approx 5000\mu_B$ at 40 K. In Ref. 19, the moment of large clusters, responsible for the nonequilibrium magnetization, was estimated in a quite different way to be $7000\mu_B$.

Now let us draw attention to the region $T>55$ K where the behavior of magnetization is of quite different kind: magnetization is almost independent of T (Fig. 4) and grows with increasing x above the point $x\approx 0.39$ (Fig. 3). The small contribution to magnetization, weakly dependent on temperature, should be assigned to very large FM clusters (called below the giant ones). The magnetic moment of a giant cluster, $m_{\rm gia}$, can be estimated from below with regard to thermodynamic equilibrium which for sure exists above 50 K. As it can be seen from Fig. 4 of Ref. 19 for all the oxygen indices, magnetization decreases less than by 10% as temperature raises from 55 to 75 K, that is by 35%. It follows from Eq. (2) that such slow temperature variation of magnetization corresponds to the region $m_{\rm gia}H/T>4$. At $H = 200$ Oe and T = 60 K, we obtain $m_{\rm gia}>2\times 10^4\mu_B$ so that a giant cluster involves more than 10^4 copper ions.

To all appearance, very large clusters are much more stable than normal-size ones and manifest themselves in high-temperature tails of magnetization (Fig. 4) as well as in the metal phase where the normal-size clusters contribution to magnetization strongly diminishes. In particular, giant clusters seem to be responsible for the residual magnetization observed in the superconducting phase above T_c (Fig. 5). The stability of very large clusters is originated by their large bond energy (see Sec. III and Sec. IV). In Sec. II C it will be shown that the giant clusters manifest themselves also under photoillumination.

The volume concentration of clusters, i.e., their contribution to magnetization divided by the cluster moment, can be estimated to be 3×10^{19} cm^{-3} (or 5×10^{-3} per unit cell) for normal-size clusters; 3×10^{17} cm^{-3} (or 5×10^{-5} per unit cell) for large clusters; and less than 2×10^{16} cm^{-3} (or 3×10^{-6} per unit cell) for giant clusters. In such a low concentration, the large and giant clusters for sure cannot manifest themselves in transport properties.

C. Anomalous effect of photoillumination on magnetization

For the elaboration of the adequate theory of FM clusters, it is of principal importance to trace the variation of magnetization with an increase of the number of holes per unit volume, n_h. In the experiments described in Sec. II A and Sec. II B the n_h varies with oxygen index x when changing from sample to sample. In the experiments described below the n_h increases in the same sample via illumination by visible light [in the insulating phase, the illumination produces a noticeable increase of n_h Refs. 26–28].

For the experimental studies of the effect of photoillumination on the magnetic properties of $YBa_2Cu_3O_{6+x}$ films, we used the samples with x close to the point of the metal-insulator transition ($x_c\approx 0.42$). Just in the vicinity of this point, the strongest change in the electrical conductivity of $YBa_2Cu_3O_{6+x}$ films under photoillumination is observed,[23] and noticeable variations in their magnetic properties can be expected.

The experiments were carried out on the films with oxygen content $x\approx 0.39$ and 0.41. The samples were illuminated by a He-Ne laser with wavelength $\lambda = 633$ nm. The light flux density at the sample was about 0.1 W/cm^2. In order to attain a uniform illumination of the sample, the laser beam was broadened. The exposure time was varied from 1 to 6 h and the illumination dose from 10^{21} to 6×10^{21} photons/cm^2, respectively. The main changes in the magnetic properties of the examined films were observed during the first hour of illumination.

The films were exposed to light at room temperature and then placed in SQUID magnetometer and cooled down to the required temperature. The time between the end of exposure and the moment when the sample reached the temperature below 200 K did not exceeded 15 minutes. This was negligibly small as compared to the relaxation time of photoinduced changes in electrical conductivity (it exceeds 10 hours at room temperature and significantly increases with lowering temperature[23]).

Figure 6 shows the $M(H)$ dependences for the films with $x\approx 0.39$ and 0.41, measured at $T=20$ K in the field parallel to c axis before and after the 6 hours photoillumination. As it can be seen in the figure for the film with $x\approx 0.39$, the magnetization curves before and after illumination practically coincide for $H<5$ kOe but drastically differ in the region $H>10$ kOe, where the magnetic susceptibility $\chi=dM/dH$ of the film threefold diminishes (from 6×10^{-4} to 2×10^{-4}) upon illumination.

For the film with $x\approx 0.41$, photoinduced changes in the $M(H)$ dependence are observed in the whole region of applied fields. In strong fields ($H>17$ kOe), photoinduced changes are similar to those for the case $x\approx 0.39$ (χ diminishes due to illumination from 2×10^{-4} to 5×10^{-5}). But in lower fields, the magnetization grows upon illumination by a value almost independent of temperature.

As an example, Fig. 7 shows $M_{\rm ZFC}(T)$ dependences measured for the film with $x\approx 0.41$ in the field $H=6$ kOe (parallel to the c axis) before and after illumination. Contrary to the initial magnetization which noticeably depends on tem-

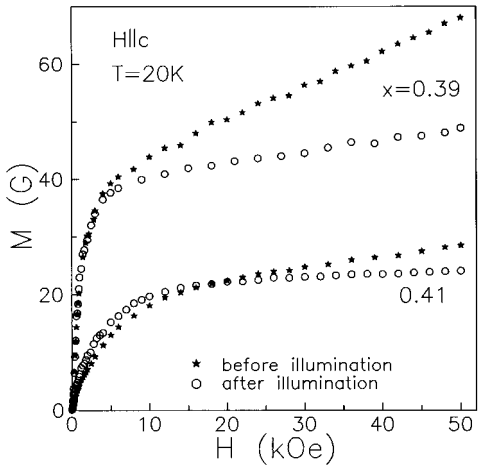

FIG. 6. Field dependences of magnetization of the $YBa_2Cu_3O_{6+x}$ films with $x \approx 0.39$ and $x \approx 0.41$, measured before and after illumination for 6 h.

perature, the photoinduced addition to $M_{ZFC}(T)$ amounts to a practically constant value of about 12 G which is of the order of the initial magnetization. In the lower field $H = 200$ Oe the photoinduced effect displays the same qualitative features: the illumination results in a temperature independent augmentation to magnetization near to 1 G, or 20 to 30% of its initial value.[19]

With regard to its very weak temperature dependence, the photoinduced addition to magnetization at $x \approx 0.41$ should be assigned mainly to the contribution of giant clusters. This suggestion is based on a large binding energy of a giant cluster which, on one hand, impedes its destruction when raising temperature and, on the other hand, originates its very great equilibrium size exceeding the real one. Under illumination the system approaches equilibrium and giant clusters grow (these mechanisms are considered in Sec. IV). At $x \approx 0.41$ such photoinduced growth of giant clusters reveals itself quite distinctly (Fig. 7), but at $x \approx 0.39$ their number is too small for noticeable manifestations under illumination.

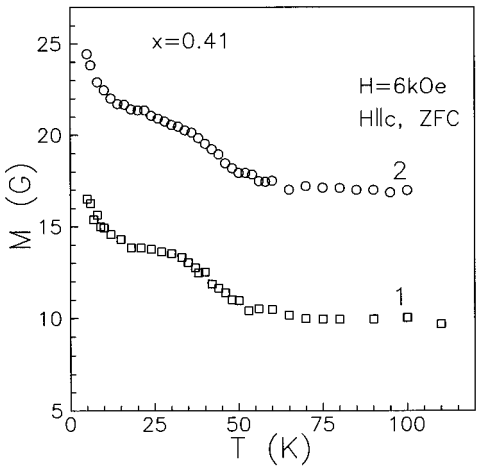

FIG. 7. Temperature dependences of ZFC magnetization of the $YBa_2Cu_3O_{6+x}$ film with $x \approx 0.41$. The dependences 1 and 2 were measured before and after illumination for 6 h, respectively. The measurements were carried out in the field $H = 6$ kOe applied parallel to the c axis.

Note that the photoinduced growth of magnetization, presented in Fig. 7 at 20 K, noticeably exceeds the corresponding quantity plotted in Fig. 6 for $x \approx 0.41$ and $H = 6$ kOe. This discrepancy is due to nonequilibrium phenomena typical of large clusters (Sec. II B) and, all the more, of giant ones (the magnetic states, presented in Figs. 6 and 7, differ by their past history).

D. Summary of the observed regularities which cannot be explained within the phase separation approach

(i) As was shown in Sec. II A, the linear field dependence of magnetization in strong fields, the slope of which is almost independent of temperature (Fig. 1), cannot be assigned to the AFM phase or to any paramagnetic contribution or paraprocess.

(ii) Magnetic susceptibility, related to FM clusters, fast grows with oxygen index up to $x \approx 0.3$, becomes almost independent of x in the interval $0.3 \leqslant x \leqslant 0.39$ and sharply decreases with raising x above ≈ 0.41. However, susceptibility contains a small contribution (almost independent of temperature and related to giant clusters) which generally grows with x in the whole interval of concentration. The nonmonotonic x dependence of susceptibility, drastically different from a fast monotonic concentration growth of the number of holes, cannot be completely assigned to the destruction of FM clusters by a percolation mechanism,[13] which begins to manifest itself near the insulator-metal transition point $x \approx 0.42$.

(iii) Photoillumination of a sample results in an essential diminution of magnetic susceptibility in the region of strong fields despite an increase in the number of holes. But at $x \approx 0.41$, susceptibility in low fields grows due to illumination.

The enumerated features can be explained with allowance for the motion of holes in long-distance potential wells (Sec. IV).

III. THE SIMPLEST THEORY OF FERROMAGNETIC CLUSTERS FORMED IN LONG-DISTANCE POTENTIAL WELLS

(1) First we consider the formation of a separate FM cluster. For $YBa_2Cu_3O_6$ ($x = 0$), copper spins are antiferromagnetically ordered within the CuO_2 plane with the exchange integral $J_{AFM} \sim 0.1$ eV. With an increase of x, in the CuO_2 plane oxygen holes appear and originate FM ordering. If one hole is fixed on an oxygen ion, two adjacent copper ions gain the effective exchange between each other, J_{FM}, amounting to a few electron volts and meeting the inequality

$$J_{AFM} \ll J_{FM} \tag{3}$$

(J_{AFM} and J_{FM} are positive quantities and the sign of the exchange energy is indicated explicitly).

The subsystem of N copper ions, perturbed by one hole fixed on an oxygen ion, contains one two-site FM cluster and has the magnetic ordering energy $E_M = -NJ_{AFM} - J_{FM} + 2J_{AFM} \approx -NJ_{AFM} - J_{FM}$. For ν fixed noninteracting holes ($\nu \ll N$),

$$E_M = -NJ_{\mathrm{AFM}} - \nu J_{\mathrm{FM}}. \quad (4)$$

Now we let oxygen holes freely move within the N-atomic subsystem (effective mass of a hole is near to unity[21]). For simplicity, we assume the holes to be uniformly distributed over oxygen ions and neglect boundary effects. Then the system is in a spatially homogeneous state which can be either antiferromagnetic with the ordering energy $E_{\mathrm{AFM}} = -NJ_{\mathrm{AFM}}$ or ferromagnetic. In the latter case the FM contribution to energy is the same as in Eq. (4) and the AFM contribution changes sign; so the total magnetic ordering energy is $E_{\mathrm{FM}} = NJ_{\mathrm{AFM}} - \nu J_{\mathrm{FM}}$. Hence the formation of the N-site FM cluster is attended by the energy change

$$E_{\mathrm{clu}} = -2N[(\nu/2N)J_{\mathrm{FM}} - J_{\mathrm{AFM}}]. \quad (5)$$

The formation of the FM cluster is energetically favorable if the concentration of holes is large enough that

$$(\nu/2N)J_{\mathrm{FM}} > J_{\mathrm{AFM}}. \quad (6)$$

If the total CuO_2 plane is considered as a homogeneous N-site system then the condition (6) cannot be fulfilled because of a small concentration of holes (less than 0.01 in the insulating phase). However, holes can be concentrated within some smaller N-site regions so that the system meets the condition (6) and gains a negative energy addition through the formation of FM clusters; the rest of the CuO_2 plane, depleted in holes, retains the AFM ordering with the unchanged energy. Within the approach of electronic phase separation such redistribution of holes is impeded by the attendant raise of Coulomb energy. But within the theory of the impurity phase separation this difficulty is deleted by the simultaneous redistribution of ionic charges.[16]

In our case, this scheme is modified: excess oxygen ions form charged copper-oxygen chains in the CuO_x plane irrespectively of the magnetic ordering in the CuO_2 plane. The chains create long-distance potential wells for oxygen holes where they are concentrated and localized. We will show that the behavior of localized holes originates the illusive anomalies stated in Sec. II D.

At first we consider a separate long-distance potential well, occupied by ν holes and involving N copper ions in the CuO_2 plane ($\nu \ll N$). If the condition (6) is met then the N copper spins are orientated parallel to each other and antiparallel to the common direction of the ν hole spins. The spin polarization of the ν holes is for sure energetically favorable since it entails the energy gain per hole ($-J_{\mathrm{FM}}$) much exceeding in magnitude the attendant raise, $\Delta\epsilon_F$, of the Fermi energy of holes [$\Delta\epsilon_F$ is of the order of the Fermi energy itself which amounts to about 0.2 eV Ref. 29]. The size of a FM cluster, estimated in Sec. II A as 80 copper ions, roughly corresponds to the area of a long-distance well.

At low temperatures the temperature dependence of m_{clu} can be linearized in T:

$$m_{\mathrm{clu}}(T) = m_{\mathrm{clu}}(0)(1 - T/T_0). \quad (7)$$

T_0 is determined by the easiest way of the destruction of a FM cluster which consists in the spin depolarization of holes occupying the highest levels of the long-distance well. This process is attended by a small energy raise if the spatial extent of a high- energy hole exceeds the cluster size (determined by the extent of the majority of localized holes). As it is seen in Fig. 1, for normal-size clusters (with $N \approx 100$) T_0 is rather small (roughly 200 K). But when applied to very large clusters (called the giant clusters in Sec. II B) this easy mechanism of destruction does not work since the spatial extent of all the localized holes is near to the size of the corresponding broad potential well. Due to this, a very large cluster has a great binding energy which promotes its thermal stability and a growth under photoillumination (Sec. II B and Sec. II C).

The contribution of all the clusters to magnetization in magnetic field, under equilibrium conditions, is described by the well-known classical formula (2). As temperature raises, the magnetization diminishes, first, due to the destruction of a cluster [described by Eq. (7)], and second, through thermal disorientation of clusters [described by Eq. (2)].

(2) Now we take account of the interaction between FM clusters caused by a weak overlapping of the hole states localized in adjacent long-distance wells A and B. Let $\mathbf{n}_A$ stand for the common unit vector of the spins of A holes and $\mathbf{n}_B$ for that of B holes. The exchange energy W_{AB}, originated by the A-B overlap of the hole wave functions, is positive for $\mathbf{n}_A = \mathbf{n}_B$ and negative for $\mathbf{n}_A = -\mathbf{n}_B$; it can be presented in the conventional form $W_{AB} = W\mathbf{n}_A\mathbf{n}_B$. Taking into account that the magnetic moment of the A or B cluster is antiparallel to $\mathbf{n}_A$ or $\mathbf{n}_B$, one can write down the energy of two interacting clusters in the magnetic field H:

$$E_{AB} = m_{\mathrm{clu}}\mathbf{H}(\mathbf{n}_A + \mathbf{n}_B) + W\mathbf{n}_A\mathbf{n}_B. \quad (8)$$

One can estimate the magnetic field, $H_0(W)$, capable of orientating both the moments, $\mathbf{m}_A$ and $\mathbf{m}_B$, in the same direction: $H_0(W) \sim W/M$. For the characteristic exchange energy $W \sim 0.1$ eV, $H_0(W) \approx 60$ kOe.

The drastically different slopes of the field dependence of magnetization in the regions of weak and strong fields can be attributed to the groups of noninteracting and interacting clusters, respectively. The first group is formed in long-distance potential wells far enough from their neighbors; such clusters are easily orientated by magnetic field according to Eq. (2).

The observed slope of the field dependence of magnetization in the region of strong fields is caused by the interactions between clusters with the overlapping energies W distributed in some interval $0 < W < W_{\max}$ ($W_{\max} > 0.1$ eV). These FM clusters begin to contribute to magnetization as H increases up to the value $H_0(W) \sim W/M$ which is distributed in the corresponding interval $0 < H_0 < H_{0\max}$ with $H_{0\max} = W_{\max}/M > 60$ kOe. This mechanism is weakly sensitive to the field direction and temperature in accordance with experiment.

First we consider the field dependence of magnetization at zero temperature. The energy (8) achieves minimum if the cluster moments lie in one plane with the vector $\mathbf{H}$ and form equal angles with it. At the point of the minimum, the energy of two interacting clusters and their total moment (directed parallel to the field) are

$$E_{AB}=-(m_{\rm clu}H)^2/2W-W,$$

$$m_{AB}=m_{\rm clu}{}^2H/W \quad \text{for} \quad m_{\rm clu}H\leqslant 2W,$$

$$E_{AB}=-2m_{\rm clu}H+W,$$

$$m_{AB}=2m_{\rm clu} \quad \text{for} \quad m_{\rm clu}H\geqslant 2W. \tag{9}$$

To obtain magnetization, the moment (9) is to be averaged over W with the weight, $\varphi(W)$, of the distribution of cluster pairs over W. Let us use the simplest distribution function:

$$\varphi(W)=\text{const}[\,\delta(W)+\gamma/W_{\rm max}] \quad \text{for} \quad W\leqslant W_{\rm max},$$

$$\varphi(W)=0 \quad \text{for} \quad W>W_{\rm max} \tag{10}$$

(γ is the ratio of the total number of interacting clusters to that of noninteracting ones). Then magnetization equals

$$M(H,T=0)=\int_0^{W_{\rm max}}\varphi(W)m_{AB}(W)dW$$
$$=nm_{\rm clu}[1+(\gamma m_{\rm clu}H/2W_{\rm max})\ln(2eW_{\rm max}/m_{\rm clu}H)]. \tag{11}$$

Equation (11) is applicable for $H\leqslant 2W_{\rm max}/m_{\rm clu}$ [at larger H magnetization remains equal to the saturation value $nm_{\rm clu}(1+\gamma)$].

In the case of a nonzero temperature, the temperature-dependent cluster moment (7) should be substituted for $m_{\rm clu}$ in Eq. (11). Besides, the thermal disordering of cluster moments is to be allowed for. When applied to the group of noninteracting clusters, this is achieved via substituting their contribution, $nm_{\rm clu}$, by the expression (2).

For the group of interacting clusters, the rigorous allowance for thermal disordering is rather a complicated procedure which is hardly reasonable with regard for a model character of the consideration in whole. Instead of this, the effect of thermal disordering can be taken into account in a simple approximate way. For a given H, the disordering of a pair of interacting clusters becomes essential in the region of large W where the magnetic ordering energy, $E_{\rm ord}=-(m_{\rm clu}H)^2/2W$, is comparable with T. Equating $E_{\rm ord}$ to bT with $b\sim 1$, we obtain the upper boundary, W_T, of the W region where cluster moments are orientated by magnetic field:

$$W_T=(m_{\rm clu}H)^2/2bT \quad (b\sim 1). \tag{12}$$

The integration over W in Eq. (11) must be restricted to the interval $0\leqslant W\leqslant W_T$ if $W_T<W_{\rm max}$. As a result, magnetization at a nonzero temperature takes up the form

$$M(H,T)$$
$$=M_0(1-T/T_0)[\coth(h/T)-T/h+(\gamma h/2W_{\rm max})\ln\xi], \tag{13}$$

where

$$M_0=nm_{\rm clu}(0), \quad h=Hm_{\rm clu}(T)=Hm_{\rm clu}(0)(1-T/T_0),$$

$$\xi=eh/bT \quad \text{if} \quad h^2/2bT\leqslant W_{\rm max},$$

$$\xi=2eW_{\rm max}/h \quad \text{if} \quad h^2/2bT\geqslant W_{\rm max} \quad \text{but} \quad h\leqslant 2W_{\rm max}.$$

The magnetization (13) achieves saturation at $h=2W_{\rm max}$ and remains constant at $h>2W_{\rm max}$.

IV. COMPARISON OF THE THEORY WITH EXPERIMENT AND EXPLANATION OF EXPERIMENTAL REGULARITIES

Section II D enumerates experimental features incomprehensible within the approach of phase separation. Now we will consider these regularities in the same sequence and explain them on the basis of the theory described in Sec. III with allowance for the behavior of holes localized in long-distance potential wells.

(i) *Field and temperature dependences of magnetization.* Let us compare the expression (13) with the experiment at the concentration point $x\approx 0.39$. The best agreement is achieved with the following values of parameters: $m_{\rm clu}=2.6\times 10^{-18}$ G cm^3, $M_o=41$ G, $T_o=233$ K, $\gamma=5$, and $W_{\rm max}=1$ eV. Here the $m_{\rm clu}$ value has an effective meaning: it makes allowance for large clusters (Sec. II B) but is much nearer to the moment of predominating normal clusters (estimated in Sec. II A as 1.4×10^{-18} G cm^3).

The dependence (13) with these values of the parameters is plotted in Fig. 1 by solid lines. As it is seen in the figure, Eq. (13) describes main experimental regularities. A fast increase of magnetization with H, observed in the region of low fields, is described by the first and second terms in square brackets, and a slow increase of magnetization in the region of strong fields is described by the last term. Some discrepancy of Eq. (13) with the experiment is due to the linear temperature expansion (7) of the cluster moment and to neglecting the nonequilibrium contribution of large clusters (Sec. II B).

(ii) *The concentration evolution of magnetization curves.* As oxygen content, x, increases, the number of holes n_h grows simultaneously with the length of the charged copper-oxygen chains, allocated in the CuO_x plane and producing wide potential wells in the CuO_2 plane (see Sec. I). Therefore, an increase in x is attended by the enhancement of the overlap of hole states localized in adjacent wide wells. This entails a decrease in the number of clusters which can be orientated by a given field H. In the concentration interval $x\leqslant 0.3$, the overlapping effect is not very significant, and magnetic susceptibility in the whole region of applied fields increases with x due to an increase of n_h. But above the concentration point $x\approx 0.3$, the overlapping grows with x very fast and originates a decreasing x dependence of susceptibility demonstrated by Fig. 3.

In the insulator-metal transition vicinity, besides this effect, the overlap of hole wave functions becomes strong enough to cause destruction of FM clusters. Indeed, if spin-polarized holes, localized in the potential well A, noticeably penetrate to an adjacent well B with the opposite direction of hole spin polarization, then A holes partially compensate the

action of B holes organizing the B cluster. Simultaneously copper ions, lying within the B well, endeavor to change the polarization direction of A holes. A diminution of the B cluster and a partial spin depolarization of A holes, originated by the former and latter effects, respectively, are enhanced by each other.

Destruction of FM clusters through hole states' overlapping should be considered as a particular case of the percolative destruction mechanism explored for $La_2CuO_{4+\delta}$ crystals.[13,30]

Such destruction mechanism seems to affect the cluster bond energy even in the insulating phase near the insulator - metal transition. Indeed, at the concentration point $x \approx 0.41$ magnetization diminishes with raising temperature much faster than at $x \approx 0.39$.[19]

Thus, near and above the insulator-metal transition point magnetization is diminished by both the mechanisms originated by the overlap of hole states localized in adjacent minima of the long-distance potential. One of the mechanisms (manifesting itself also at lower concentrations) impedes FM clusters to be orientated by magnetic field and the second destroys the clusters. Due to the simultaneous action of the mechanisms, only a small contribution of giant clusters persists in the metal phase (this is evidenced by the comparison of Figs. 4 and 5).

In the case of very large clusters the overlapping effect is much weaker for the following reasons. First, the magnetic moments of giant clusters are much easier orientated by field than those of normal clusters for the same overlap energy W. Second, for a very large area of adjacent wells, W is small since the normalized wavefunction of a localized hole has a very weak tail beyond the well. Due to this, the contribution of giant clusters to magnetization generally grows with x up to the point $x \approx 0.44$. Such x-dependent contribution of giant clusters reveals itself in high temperature range (Figs. 3, 5, and 7) and in the total region of temperatures as a photoinduced augmentation of magnetization (Fig. 7).

(*iii*) *The effect of photoillumination.* The illumination of YBCO films affects magnetic structure via two competing mechanisms. First, photoillumination produces an increase in the number of holes which is noticeable for small x (for instance, the photoinduced increase in the conductivity of the sample with $x \approx 0.39$ amounted to about 25% at room temperature). Second, photoillumination causes the lengthening of copper-oxygen chains,[28,31] which entails an enhancement of the overlap between the hole states, localized in adjacent wells, and the corresponding decrease of susceptibility. Since the overlap is highly sensitive to the shape of the long-distance potential, the second effect generally predominates and results in a significant diminution of susceptibility in the range of strong fields where susceptibility is determined by the overlapping.

But in the range of low fields, the first mechanism compensates the second one at $x \approx 0.39$ (Fig. 6) or even noticeably predominates at $x \approx 0.41$ (Figs. 6 and 7). This feature should be attributed mainly to giant clusters which are not very sensitive to the overlapping effect [see item (ii)]. A giant cluster is a firmly bound system weakly sensitive also to thermal disordering (see Sec. III); therefore, the contribution of giant clusters to magnetization is almost independent of temperature. For instance, Fig. 7 demonstrates the constancy of the photoinduced augmentation of magnetization, originated by giant clusters, when raising temperature. Their contribution reveals itself also before illumination as a background almost independent of temperature.

The photoinduced growth of giant clusters is promoted by their large bond energy and realized through the growth of copper-oxygen chains in the CuO_x plane. Such a chain, producing the potential well where holes concentrate, is a constituent of a cluster; it grows under illumination since a giant cluster has a great bond energy and its enlarging is thermodynamically favorable. Illumination accelerates the diffusion of oxygen ions in the CuO_x plane which results in approaching equilibrium.

These considerations explain why the temperature independent contribution to magnetization becomes noticeable as a high enough oxygen content ($x \geqslant 0.41$) provides the existence of a sufficient amount of giant clusters (Fig. 7). In the metal phase normal clusters do not contribute to magnetization due to a strong overlap effect, but giant clusters still produce magnetization weakly dependent on T (Fig. 5).

V. CONCLUSION

There are unambiguous experimental evidences for the formation of FM clusters in YBCO antiferromagnetic insulators. The clusters are formed by the concentration of holes in a general accordance with the phase separation approach. However, field and concentration dependences of magnetization display some essential features (Sec. II D) which can be explained only by taking into account the detailed behavior of holes in long-distance potential wells. In that way the following physical pattern was developed.

An FM cluster is formed in the CuO_2 plane by oxygen holes, localized in a long-distance potential well, involving a few hundreds of the plane lattice sites. Such potential wells exist independently of the magnetic structure; they are created in the CuO_2 plane by charged copper-oxygen chains, formed in the CuO_x plane by a physical-chemical mechanism, bearing no direct relation to magnetic ordering.[20,28,32] An extremely low mobility of oxygen ions, belonging to the copper-oxygen chains, is evidenced by their large relaxation time (several hours even at room temperature.[22]) This results in a high stability of the long-distance potential relief and in a negligibly low mobility of FM clusters formed in its minima.

For comparison it should be mentioned that in $La_2CuO_{4+\delta}$ crystals, where FM clusters are also formed in the CuO_2 plane by oxygen holes, the holes concentrate simultaneously with the FM cluster formation and the rearrangement of mobile oxygen ions in the La_2O_2 plane. In that case FM clusters have a noticeable mobility commensurate with the mobility of oxygen charges in the La_2O_2 plane.[13]

There is a significant straggling of the clusters over sizes. For normal (predominating) clusters, containing about 100 copper spins, the bond energy amounts roughly to 200 K. Giant clusters (involving above 10^4 spins) are bound much stronger, and their contribution to magnetization is almost independent of temperature and persists with raising x even in the metal phase.

Field and concentration dependence of the FM cluster behavior is to a great extent dictated by the overlap of hole

states, localized in adjacent long-distance potential wells, which makes the opposite orientations of their spins energetically favorable. To orientate parallel the spins together with the corresponding cluster moments, a strong enough field is required. This results in the nearly linear field dependence of magnetization in a wide region of strong magnetic fields. With raising oxygen index the overlapping effect grows and near the insulator-metal transition not only diminishes magnetization but also begins to destroy FM clusters. Due to this, only a small contribution of giant clusters (weakly sensitive to the overlapping effect) persists in the metal phase.

The distribution of clusters over sizes seems to be structure sensitive and to mirror the inhomogeneity of samples. So, magnetic measurements can be used for nondestructive control of samples.

[1] H. Kadowaki, M. Nishi, Y. Yamada, H. Takei, S.M. Shapiro, and G. Shirane, Phys. Rev. B **37**, 7932 (1988).

[2] J. M. Tranquada, G. Shirane, B. Keimer, S. Shamoto, and M. Sato, Phys. Rev. B **40**, 4503 (1989).

[3] W. E. Farneth, R. S. McLean, E. M. McCarron, F. Zuo, Y. Lu, B. R. Patton, and A. J. Epstein, Phys. Rev. B **39**, 6594 (1989).

[4] Y. Yamaguchi, S. Waki, and M. Tokumoto, Solid State Commun. **69**, 1153 (1989).

[5] H. Theuss and H. Kronmuller, Physica C **178**, 37 (1991).

[6] X. Obradors, J. Tejada, J. Rodriguez, F. Peres, M. Vallet, J. Gonzalez-Calbet, and M. Medarde, J. Magn. Magn. Mater. **83**, 517 (1990).

[7] T. Ishii, T. Yamada, K. Sugiyama, H. Fuke, and M. Date, Physica C **165**, 139 (1990).

[8] F. Zuo, A. J. Epstein, E. M. McCarron, and W. E. Farneth, Physica C **167**, 567 (1990).

[9] V. J. Emery, Phys. Rev. Lett. **58**, 2794 (1987).

[10] A. Aharony, R. J. Birgeneau, A. Caniglio, M. A. Kastner, and H. E. Stanley, Phys. Rev. Lett. **60**, 1330 (1988).

[11] M. M. Bogdan and A. S. Kovalev, Fiz. Nizk. Temp. **16**, 1576 (1990) [Sov. J. Low Temp. **16**, 887 (1990)].

[12] V. Hizhnyakov and E. Sigmund, Physica C **156**, 655 (1988).

[13] E. Sigmund, V. Hizhnyakov, R. K. Kremer, and A. Simon, Z. Phys. B **94**, 17 (1994).

[14] V. J. Emery, S. A. Kivelson, and H. Q. Lin, Phys. Rev. Lett. **64**, 475 (1990).

[15] E. L. Nagaev, Zh. Eksp. Teor. Fiz. **103**, 252 (1993) [JETP **16**, 138 (1993)].

[16] E. L. Nagaev, Usp. Fiz. Nauk **165**, 528 (1995).

[17] *Phase Separation in Cuprate Superconductors*, edited by E. Sigmund and K. A. Muller (Springer-Verlag, Berlin, 1994).

[18] R. Szymczak, H. Szymczak, and S. Piechota, Z. Phys. B **99**, 25 (1995).

[19] S. L. Gnatchenko, M. Baran, R. Szymczak, and H. Szymczak, Fiz. Nizk. Temp. **21**, 1157 (1995) [Low Temp. Phys. **21**, 888 (1995)].

[20] G. Uimin and J. Rossat-Mignod, Physica C **199**, 251 (1992).

[21] A. M. Ratner, Fiz. Nizk. Temp. **21**, 208 (1995) [Low Temp. Phys. **21**, 159 (1995)].

[22] V. M. Dmitriev, V. V. Eremenko, I. S. Kachur, V. G. Piryatinskaya, O. R. Prikhod'ko, A. M. Ratner, E. V. Khristenko, and V. V. Shapiro, Fiz. Nizk. Temp. **21**, 219 (1995) [Low Temp. Phys. **21**, 168 (1995)]; V. V. Eremenko, I. S. Kachur, V. G. Piryatinskaya, A. M. Ratner, and V. V. Shapiro, Physica C **262**, 54 (1996).

[23] V. I. Kudinov, I. L. Chaplygin, A. I. Kirilyuk, N. M. Kreines, R. Laiho, E. Lahderanta, and C. Ayache, Phys. Rev. B **47**, 9017 (1993).

[24] R. J. Cava, B. Batlog, K. M. Rabe, E. A. Rietman, P. K. Gallagher, and L. W. Rupp, Physica C **156**, 523 (1988).

[25] H. Theuss and H. Kronmuller, Physica C **177**, 253 (1991).

[26] J. Smart, *Effective Field Theories of Magnetism* (W. B. Saunders Company, Philadelphia-London, 1966).

[27] G. Yu and A. J. Heeger, Int. J. Mod. Phys. B **7**, 3751 (1993).

[28] G. Nieva, E. Osquiguil, J. Guimpel, M. Maenhoudt, B. Wuyts, Y. Bruynseraede, M. B. Maple, and I. K. Schuller, Phys. Rev. B **46**, 14249 (1992).

[29] I. Fugol', V. Samovarov, A. Ratner, V. Zhuravlev, G. Saemann-Ischenko, M. Lippert, and B. Holzapfel, Physica C **216**, 391 (1993).

[30] M. Baran, H. Szymczak, and R. Szymczak, Europhys. Lett. **32**, 79 (1995).

[31] J. Hasen, D. Lederman, I. K. Schuller, V. Kudinov, M. Maenhoudt, and Y. Bruynseraede, Phys. Rev. B **51**, 1342 (1995).

[32] B. W. Veal, H. You, A. P. Paulikas, H. Shi, Y. Fang, and J. W. Downey, Phys. Rev. B **42**, 4770 (1990).